Strategies to improve hydrogen activation on gold catalysts

Nikolaos Dimitratos, Gianvito Vilé, Stefania Albonetti, Fabrizio Cavani, Jhonatan Fiorio, Núria López, Liane M. Rossi, Robert Wojcieszak

Chemical aspects in hydrogenation on gold nanocatalysts

N. Dimitratos[1], G. Vilé[2], S. Albonetti[1], F. Cavani[1], J. Fiorio[3], N. López[4], L.M. Rossi[5], R. Wojcieszak[6,*]

[1]*Dipartimento di Chimica Industriale "Toso Montanari", Alma Mater Studiorum Università di Bologna, Viale Risorgimento 4, 40126 Bologna, Italy*
[2]*Department of Chemistry, Materials and Chemical Engineering "Giulio Natta", Politecnico di Milano, Piazza Leonardo da Vinci 32, 20133 Milano, Italy*
[3]*Technische Universität Dresden, School of Science, Faculty of Chemistry and Food Chemistry, Mommsenstr. 13, 01069 Dresden, Germany.*
[4]*Institute of Chemical Research of Catalonia, The Barcelona Institute of Science and Technology, Tarragona, Spain*
[5]*Departamento de Química Fundamental, Instituto de Química, Universidade de São Paulo, Av. Prof. Lineu Prestes 748, São Paulo 05508-000, SP, Brazil*
[6]*Univ. Lille, CNRS, Centrale Lille, Univ. Artois, UMR 8181 - UCCS - Unité de catalyse et chimie du solide, F-59000 Lille, France*

**Corresponding author. E-mail: Robert.wojcieszak@univ-lille.fr*

ABSTRACT

Catalytic transformations involving hydrogen are among the most important processes in the chemical industry. While this process occurs easily in the presence of nickel or platinum, the use of gold as an alternative catalyst has gathered significant attention only in recent years. However, the understanding of the physicochemical effects involved during hydrogen activation and reaction on gold surface or gold/support interfaces still need advances. It is important to understand how to improve the hydrogenation properties of gold, and rationally design better catalysts. In this context, this review presents a concise but complete analysis of the strategies implemented to improve hydrogen-gold interactions, from addressing the role of metal particle size, to the alternative mechanisms for molecular hydrogen (H_2) dissociation based on gold cations and gold-ligand interfaces.

1. Introduction

Heterogenous catalysts are at the heart of many industrial processes [1-3], and often involve finely dispersed metallic nanoparticles. In this context, gold nanoparticles (Au NPs) dispersed on solid carriers possess remarkable catalytic abilities [4], which have been initially demonstrated for oxidation reactions [5-8]. This is related to the presence of more low-coordination surface sites, which offers higher catalytic properties over conventional gold surfaces [7, 9]. The origin in the activity and selectivity enhancements can be traced back to dispersion and quantum effects unique to the nanoscale, leading to the emergence of unusual electronic and/or atom packing shell structures, and the interactions with the support. Therefore, it is not surprising that gold nanoparticles are able to activate small molecules such as carbon monoxide at significantly lower temperatures.

The discovery that, in some specific cases and when the metal particle size is below 10 nm, Au NPs can also dissociate molecular hydrogen, therefore showing a catalytic function in hydrogenation reactions, has broken a long-standing glass ceiling in chemistry, and has attracted attention from academia and industry [10-12]. Understanding how hydrogen can be activated with gold is essential for the rational design of efficient and stable gold catalysts for hydrogenations [13-14].

Generally, hydrogenation reactions on metal surfaces follow the Horiuti-Polanyi mechanism, that involves the homolytic splitting of H_2 and the sequentially transferring of the surface-adsorbed H atoms on the reactive molecule. This critical activation step has been demonstrated using IR, XAFS, and H/D exchange experiments on supported Au NPs [15-18]. Experimental and theoretical studies have corroborated that the active sites responsible for the dissociative adsorption of molecular hydrogen are the low-coordinated atoms located on the corner and edge of the Au NPs [19]. Some important scientific questions remain concerning the possible charge transfer between Au and H, the presence of alternative (spontaneous or

activated) hydrogen dissociation paths, and the degree of mobility of H species on the Au NPs [20]. However, the main challenge in using gold for hydrogenation reactions is intrinsically connected with its low efficiency in dissociating H_2 under standard conditions, due to the degree of filling of the antibonding states, and the degree of orbital overlap with the adsorbate [21]. This results in lower gold-catalyzed hydrogenation performance.

2. Hydrogenations on gold

Gold nanoparticles enable catalytic activation at significantly lower temperatures, e.g. in CO oxidation. The development of original gold based catalytic formulations and the enhancement of existing ones [4, 14, 22-27] both require large efforts, involving the study of the impacts of active metals, supports, solvents, metal additives, co-catalysts, catalyst preparation methods, study of active site [1] and/or the combination of all these parameters. Significant progress was made on the catalytic performances through the synthesis of multi-phase formulations (bimetallic and promoted gold catalysts) and obviously on active phase dispersion methods that act directly on the gold NPs size and localization within the support. Theoretical calculations were performed also to understand the mechanisms of H_2 activation, possible hydrides formation [28] and adsorption of the substrates on gold and oxide surfaces, while reaction mechanisms and kinetics have been elucidated over some catalytic systems. Nonetheless, the development of gold catalysts is still hampered by a series of obstacles. The control and tunability of the chemical composition of gold and gold bimetallic nanoparticles/nanoclusters are still limited when catalysts are prepared via traditional methods such as co-precipitation or co-impregnation of metal salts. These procedures often result in a poor control of the average and the distribution of the particle sizes, and the formation of a mixture of mono- and bimetallic particles even within the bimetallic systems stability domains expected from the phase diagrams. Another striking problem is the deactivation of the catalyst due to structure degradation, leaching, valence change of the gold, carbon

deposition, *etc* [29]. The mechanisms underlying the degradation of the catalyst performances are still not fully understood and most importantly not yet solved. Finally, the knowledge of fundamental aspects, including the reaction mechanisms at the molecular level, kinetic modeling, adsorption geometry of substrates on gold surface, and the active phase modeling, is far from complete.

Research in catalysis by gold was motivated by the possibility of improving the efficiency of catalytic processes by designing nanostructured catalysts that possess novel catalytic properties such as low temperature activity, selectivity, stability and resistance to poisoning and degradation. Structure-sensitivity, real structure of supported gold catalysts and attempts to identify the active sites are essentials in reactions exhibiting severe selectivity problem. The main characteristic feature of gold catalysts is the high selectivity in hydrogenation reactions. The discovery that in some specific cases, Au NPs can dissociate molecular hydrogen when the Au particle size varies from 2 nm to 10 nm, has motivated the research in the synthesis of size and shape-controlled Au nanoparticles for hydrogenation reactions [11-12]. Dissociative adsorption of molecular hydrogen on supported Au NPs, using a range of different oxide supports has been demonstrated using IR, XAFS and H/D exchange experiments [15-18]. Moreover, experimental and theoretical studies have shown that the active sites responsible for the dissociative adsorption of molecular hydrogen are the low-coordinated atoms located on the corner and edge of the Au NPs [19]. Even if the mechanism of H_2 dissociation on gold surface is well established from the computational point of view, the fate of the H atoms is still not completely understood. For example, discrepancies exist regarding which atoms of the gold NPs are specifically the most reactive, whether there is a charge transfer between Au and H, whether the dissociation is spontaneous or activated, and finally the degree of mobility of H atoms on the Au NPs [20]. Theoretical investigations helped in developing of more efficient gold-based catalysts for this process, open surfaces as

Au(100) and low coordinated sites enhance the gold activity irrespective whether if they are located at the edge or belong to an extended line defect [30]. A fundamental understanding of the hydrogen interaction [31] with gold and the role of metal-ligand and metal-support interaction in gold catalysis is important to rationalize the performance of the catalysts, from the nano to the single-atom level [32-33]. In case of alkynes semihydrogenation, the higher selectivity of gold compared to palladium was predicted by DFT and then experimentally. The carbon-carbon triple bonds of alkynes are preferentially adsorbed and activated on gold, whereas carbon-carbon double bonds of alkenes are not. In contrast, both carbon-carbon triple and double bonds are adsorbed on palladium. Thus, C=C and C≡Cs compete for the active sites on Pd being hydrogenated, whereas on Au the molecules containing C=C leave the catalyst surface and where not hydrogenated [30]]. Gold also exhibited high chemoselectivity for the hydrogenation of α,β-unsaturated aldehydes to the corresponding unsaturated alcohols [34] and for the deprotection of epoxides via deoxygenation back to the corresponding alkene [35], in both cases preserving the carbon-carbon double bonds.

The semi-hydrogenation of alkynes is one of the most straightforward methods for the synthesis of alkenes using H_2 as the hydrogen source. Pd-based nanoparticles have shown high catalytic efficiency; however, the main obstacles are the over-reduction to alkanes and C-C coupling leading to coke formation, therefore a lower selectivity towards to alkenes. On the other hand, supported gold nanoparticles are promising catalysts due to the fact that gold nanoparticles are alkynophiles, whereas in the case of Pd, there is no differential adsorption of alkene and alkyne bonds and therefore can possess better selectivity. An effective process for the semi-hydrogenation of diphenylacetylene as the chosen model was demonstrated using a commercial Au/TiO_2 catalyst. The reductant molecule was ammonium formate instead of H_2 and a yield of 70% to *cis*-diphenylethene without the formation of trans-isomer at mild reaction conditions was achieved. In addition, various internal and terminal alkynes, with

either electron-donating or electron withdrawing groups, were tested and excellent yields were obtaining for cis-alkenes (76-96%). The effect of support was not crucial in terms of yield and selectivity and reusability of the catalyst was promising, showing a slow deactivation of the gold catalyst due to the mild aggregation of gold nanoparticles [36].

3. Improving the gold-hydrogen interactions:

The inability of Au to activate H_2 is the rate-determining step in gold-catalyzed hydrogenations **(Figure 1a-b)**. [21]. Several strategies exist which permit to enhance the rate of dissociation of hydrogen on gold surfaces, improving the catalytic properties of gold-based catalysts. Thus, we give herein a systematic and critical analysis of the most important approaches to enhance the reactivity of gold with hydrogen.

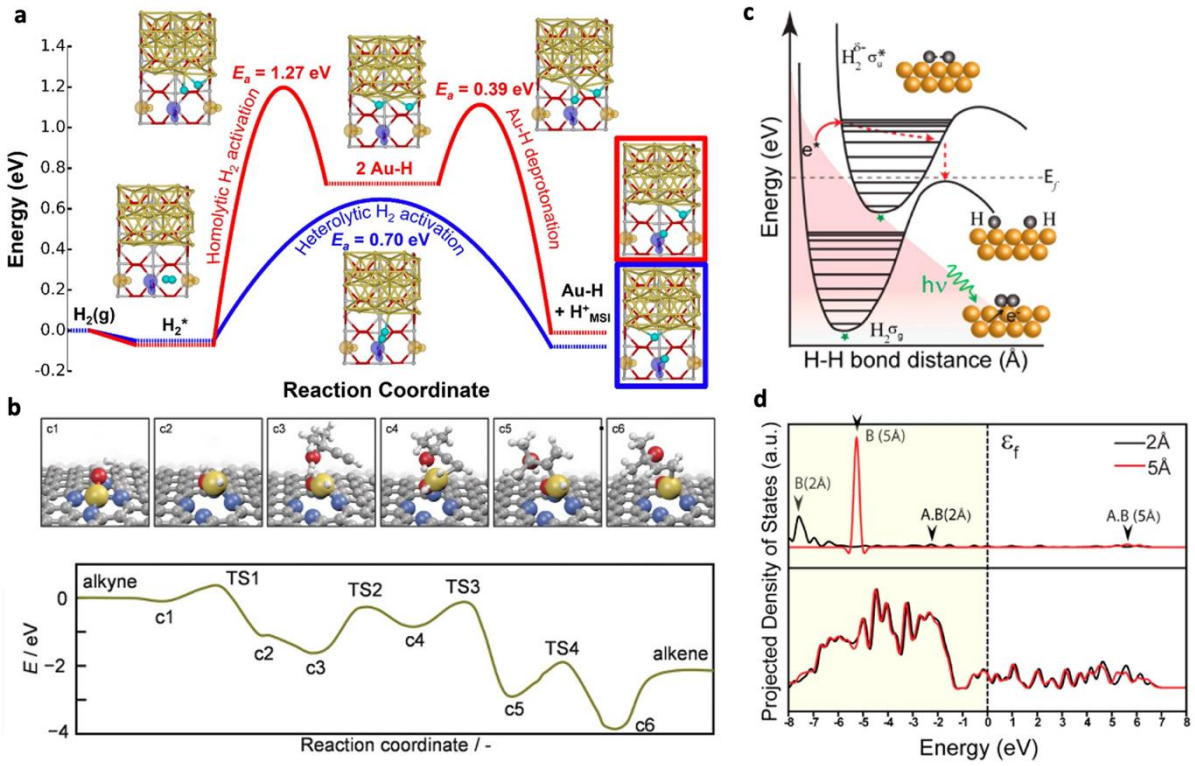

Figure 1. *Gold heterogeneous catalysts and the types of H_2 activation.* ***(a)*** *Potential energy diagram comparing the heterolytic H_2 activation across the MSI at a cus-OH site (blue) with homolytic H_2 activation on Au_{MSI} followed by deprotonation (red). H_2(g) is used as reference energy [50].* ***(b)*** *Energy profile for the hydrogenation reaction of 2-methyl-3-butyn-2-ol on a single gold atom in the oxidized-4-pyridinic cavity and side view of DFT-optimized adsorption configuration of the intermediates [51].* ***(c)*** *Proposed mechanism of hot-electron induced dissociation of H_2 on AuNP surface [55].* ***(d)*** *Electronic density of states (DOS) of H_2 approaching a Au (111) surface using DFT, at different surface distances (see inset), projected onto one approaching atomic H atom (top panel) and total DOS (bottom panel). H_2 bond length is 0.725 Å. The dashed line marks the Fermi energy. Arrows denote the bonding (B) and antibonding state (AB) of H_2. [51]*

3.1. Ligands

The addition of a ligand to a Au NPs is one of the possibilities to improve the hydrogenation ability of this metal. For example, it has been shown that Au NPs embedded in a N-doped carbon activate H_2 with an energy barrier of 1.45 eV, and the reaction energy is endothermic by 0.69 eV [37]. However, when the same gold nanoparticle is decorated with 1,10-phenanthroline to mimic graphene-like sheets, the nitrogen atoms on the ligand assisted Au in the surface activation of H_2 *via* an heterolytic path **(Figure 1c-d)**, with an energy barrier of only 0.30 eV. The intermediate formed is significantly exothermic by 0.71 eV, and the catalytic system can be rationalized as frustrated Lewis pairs (FLP) analogue [38]. The formation of FLP interface has also been demonstrated by combining Au NPS either with phosphorous- or nitrogen-containing ligands [39-41]. As verified by DFT calculations, these systems are all capable of heterolytically activating H_2. The generated hydride and proton can, for example, be concertedly transferred to CO_2 to produce formic acid [42].

The ligands can be also added directly in the reaction media. In case of selective hydrogenation of alkynes into *cis*-alkenes using molecular hydrogen, a significant promotion effect is reported when nitrogen-containing bases are used in the presence of gold nanoparticles supported on SiO_2. In fact, in the absence of nitrogen-containing bases, supported gold nanoparticles showed a poor catalytic performance with conversion below 1%. It was found that nitrogen-containing bases with two heteroatoms performed better and in the presence of piperazine, at high conversion, high selectivity to the alkene was reported, showing the best catalytic results among the amines tested. Reusability tests showed the catalyst was stable without significant leaching. Moreover, the effect of the concentration of piperazine used was studied, showing that piperazine not only facilitates the activation of Au nanoparticles as hydrogenation catalyst but it also promotes the selectivity to alkene by

avoiding the subsequent hydrogenation of alkene to alkane, therefore by tuning the substrate to piperazine molar ratio, the enhancement of activity and selectivity to the desired product is possible **(Figures 2 a-d)**. Moreover, the general applicability of the methodology was demonstrated with the efficient hydrogenation of terminal and internal alkynes with moderate to excellent yield to alkene and with minimum over-reduction to alkane. Based on the scientific findings it was suggested that the role of piperazine is to facilitate the heterolytic activation of hydrogen at the surface of Au nanoparticles, due to the fact that the nitrogen atom of piperazine can act as a basic ligand to promote the heterolytic hydrogen cleavage and therefore providing hydrogen activation at mild reaction conditions **(Figures 2 i-j)**. According to simulations, molecular hydrogen dissociation occurs at the ligand−gold interface, and the nitrogen-containing bases with two heteroatoms were more efficient to lower the energy barrier for the heterolytic H_2 dissociation and boost gold hydrogenation activity **(see Figure 1b)**. Finally, it was concluded that it is important to achieve an optimum balance of the different experimental conditions tested, and the following parameters should be considered, such as, (i) basicity of the ligand and reorganization energy of the ligand to activate hydrogen and (ii) the possibility of site blocking depending on the ligands used, and (iii) the metal leaching effect induced by some ligands for affecting activity, selectivity and stability [39].

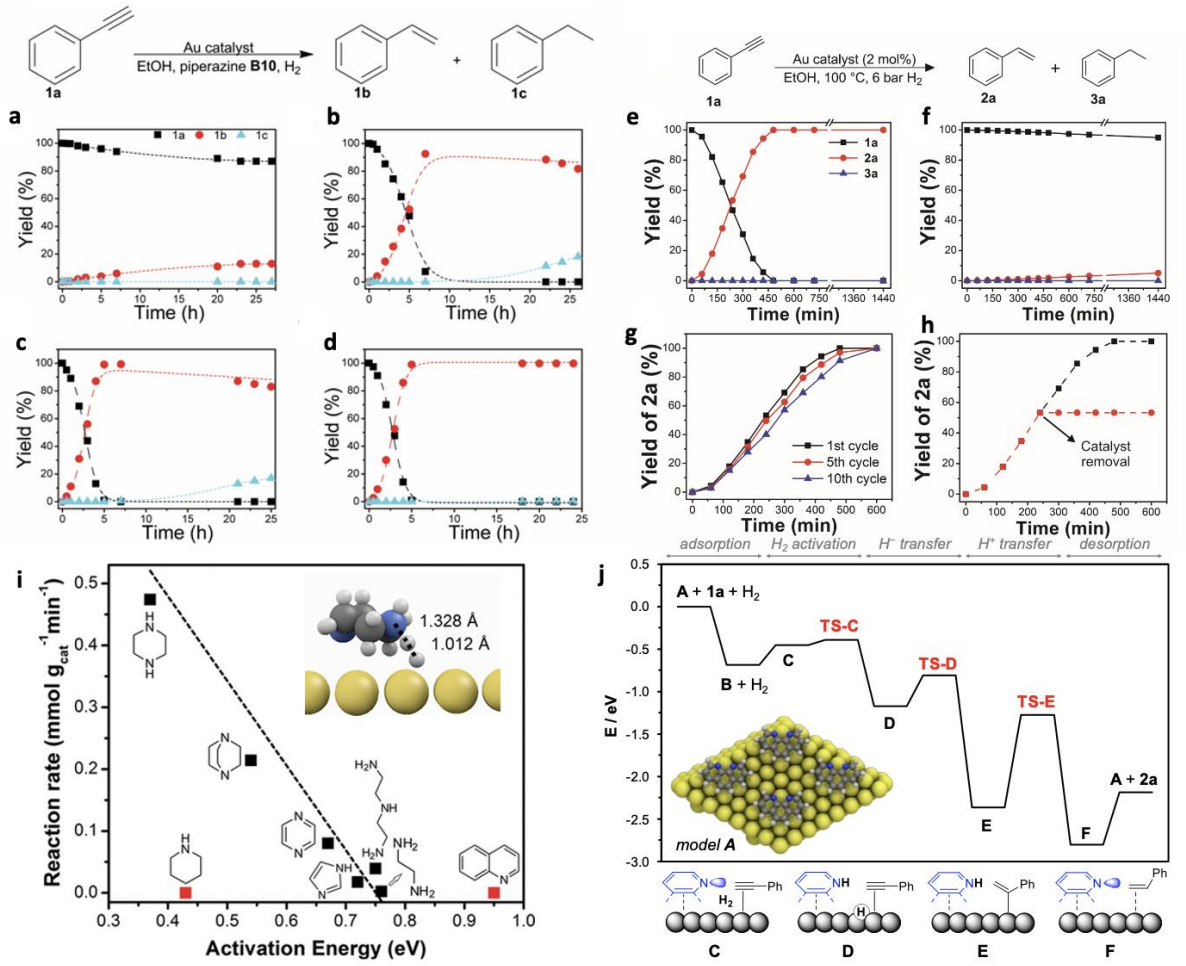

Figure 2. ***(a-d)*** *Time course of hydrogenation of phenylacetylene catalyzed by Au/SiO_2 with increasing amounts of piperazine:* ***(a)*** *0.04 mmol;* ***(b)*** *0.4 mmol;* ***(c)*** *2 mmol;* ***(d)*** *4 mmol. Reaction conditions: 4 mmol of phenylacetylene, 0.04 mmol of Au, 0.04−4 mmol of amine, 8 mL of ethanol, 80 °C, 6 bar of H_2.* ***(e-h)*** *Time course of hydrogenation of phenylacetylene catalyzed by* ***(e)*** *Au@N-doped carbon/TiO_2 and* ***(f)*** *Au/TiO_2;* ***(g)*** *recycling experiments using the Au@N-doped carbon/TiO_2; and* ***(h)*** *hot filtration test. Reaction conditions: 0.14 mmol of 1a, 2 mol% of Au, 2 mL of ethanol, 100 °C, 6 bar of H_2,* ***(i)*** *Energy profile for the hydrogenation reaction of 2-methyl-3-butyn-2-ol on a single gold atom in the oxidized-4-pyridinic cavity and side view of DFT-optimized adsorption configuration of the intermediates.* ***(j)*** *Electronic density of states (DOS) of H_2 approaching a Au (111) surface using DFT, at different surface distances (see inset), projected onto one approaching atomic H atom (top panel) and total DOS (bottom panel). H_2 bond length is 0.725 Å. The dashed line marks the Fermi energy. Arrows denote the bonding (B) and antibonding state (AB) of H_2. Reprinted with permission from [37, 39].*

Nitrogen-doped carbon materials are known to affect the catalytic activity of embedded metal nanoparticles for various reactions, including hydrogenations, where the basic N atoms of the support material may cooperate for the heterolytic activation of H_2 at the metal-N-doped carbon interface. In this context, gold nanoparticles embedded in N-doped carbon materials supported on titania (Au@N-doped C/TiO_2) showed an enhanced catalytic activity **(Figures 2 g-j)** when compared to Au/TiO_2 for alkyne semihydrogenation. The main advantage regarding the previous study where gold was activated with piperazine [39] is the catalyst reutilization **(Figure 2 i)** without the need of external ligands **(Figures 2 j)**. A

combination of experimental results and computational study **(Figures 2 k)** revealed a N-assisted heterolytic H_2 activation mechanism that boost the catalytic activity. The absence of a direct interaction between the lone pair of the nitrogen and the gold surface creates a unique interface that can be related to a frustrate Lewis pair, enabling the heterolytic activation of molecular hydrogen [37]. There are other examples in the literature on the utilization of the cooperation between gold and adsorbed basic ligands to unlock the catalytic activity of gold for hydrogenations of organic molecules, including quinoline [43], imine or nitrile [44] and secondary phosphine oxides [45-46].

3.2. Gold-support interactions

Another strategy to enhance the catalytic activity of gold is to exploit the concept of strong metal-support interaction (SMSI). The support, in fact, can stabilize dissociated hydrogen. Compared to homolytic dissociation, heterolytic dissociation is much more energy intense (4.4 eV vs 16.9 eV). Thus, the extra energy needs to be compensated by the new bonds formed upon dissociation, and this sets a minimum of charge separation that allows the process to be viable [47]. The interface of the heterogeneous oxide carrier can help enhancing the heterolytic process [48-50]. This has been demonstrated, for example, by the low coordinated oxygen atoms on TiO_2(110) close to the Au clusters, that were found to be able to cause the dissociation of H_2 and protonate the O atoms of the support [49]. In contrast, the Au SAs supported in electron-rich cavities of N-doped carbon dissociate H_2 homolytically [51]. The catalyst was suggested by DFT to be composed of $Au^{\delta+}$ ($1<\delta<3$) species stabilized in oxidized-4-pyridine cavities from the N-doped carbon. When the H_2 activation step was studied, the developed catalyst led to thermodynamically more favored step than on the stepped surface Au(211) (−1.13 eV versus −0.17 eV, respectively).

The structure-sensitivity of gold can also induce catalytic effects. The catalytic performance of Au catalysts showed that small nanoparticles around 3 nm had higher

selectivity (78%), while Au nanoparticles with mean particle size of 9 nm showed much lower selectivity (39%) in the hydrogenation of 3-nitrostyrene. A model catalyst was synthesized by depositing both 3 nm and 9 nm Au nanoparticles onto TiO_2, showing a moderate selectivity (55%) at a higher conversion. However, when a reduction process was utilized for the Au catalysts either with small or larger particle size, the selectivity was improved significantly reaching over 95%. The main difference was in terms of conversion where the catalyst with the largest Au nanoparticles (around 9 nm) exhibited a significant lower conversion, whereas Au catalysts with mean particle size of 3 nm or a combination of 3 nm and 9 nm, maintain the conversion level. By characterizing the catalysts with HRTEM it was found that the catalyst with the larger Au nanoparticles (9 nm) had a significant degree of encapsulation, therefore the catalytic activity was significant lower. In the case of smaller Au nanoparticles, were only partially encapsulated. The authors explained the observed trend, based on the fact that the encapsulation occurred during SMSI can be considered as a wetting process of the Au NPs by reduced titanium oxide) and the encapsulation process is mainly determined by the surface tensions of the metal and support. Assuming that in the scale of NP size of interest, overlayer species TiO_{2-x} are abundant, therefore at any thermodynamically equilibrated states the encapsulation degree θ is only the function of surface tensions γ_{Au}, γ_{int}, γTiO_{2-x}, and r, the radius of NP. The authors demonstrated that the surface tension increases with NP size, therefore, larger Au NPs with higher surface energy has stronger tendency to be wetted by TiO_2 and as a consequence can lead to a higher degree of encapsulation. The enhancement of the selectivity after the heat treatment with hydrogen was attributed due to the electronic effect upon reduction creating electron rich sites and the favorable adsorption of $–NO_2$ group on these sites [52].

An alternative novel strategy for enhancing the catalytic performance of gold was by using synthesized uniform gold nanoparticles with carbon atoms occupying interstitial sites in

the lattice (C–Au). The main hypothesis was that the formation of interstitial C in the Au lattice modifies its electronic properties and therefore can affect catalytic performance. The catalytic performance was investigated using synthesized and commercial catalysts. The material with interstitial C species showed an improved catalytic performance and a high selectivity (well beyond 95%). To explain the observed catalytic trend DFT and XPS studies were carried out. The formation of interstitial C in the Au lattice facilitated the heterolytic dissociation of hydrogen on C-Au due to electron transfer between C and Au and therefore improvement of catalytic activity. Moreover, the high chemoselectivity observed for the C-Au ordered mesoporous carbon catalysts (OMC) was attributed to the perpendicular adsorption, stronger interaction and activation of 3-nitrostyrene over the C-Au surfaces. It was concluded that the formation of gold nanocatalysts with C occupying interstitial sites in its lattice provides high d-electron gain and can significantly enhance the electron transfer at Au sites with a consequence the stronger adsorption and activation of the substrate on the C-Au surfaces. This enhanced H_2 dissociation and improved the catalytic performance in hydrogenation reactions [53].

3.3. Plasmon enhancement

Besides metal support interactions and ligand effects, exploiting the plasmonic properties of Au NPs is a very interesting alternative to activate H_2 [54-55]. Mechanistically, localized surface plasmons (LSPs) excited on metal NPs decay non radiatively into high energy hot electrons. These hot electrons may then relax through electron−phonon coupling or, in the presence of molecular adsorbates, may scatter into an excited state of the molecule, initiating a chemical reaction. The transfer of electrons to the antibonding orbital of H_2 molecules [55] weakens the bong strength and stretches H–H bond, thereby decreasing the barrier for its activation **(Figure 1e)**.

It was demonstrated that the hot-electron-induced photodissociation of H_2 occurred on small Au nanoparticles **(Figures 3 a-d)**. Moreover, to strengthen the evidence that dissociation is indeed taking place on the illuminated AuNP surface, mediated by hot-electron capture by the adsorbate molecules. It was also shown that when the support changed from SiO_2 to TiO_2, the rate of H_2 dissociation decreased significantly, showing that the dielectric support did not actively participate in the chemical reaction [20]. In spite of the numerous studies undertaken in this field, the issue of diffusion and recombination of the H atoms after H_2 dissociation has not been investigated thoroughly. A comprehensive investigation of these latter issues is therefore still essential for a deep understanding of H adsorption and hydrogenation reactions on the Au NPs. The adsorption and diffusion of H_2 on Au NPs followed by wavelength shift of the localized surface plasmon resonance (LSPR) displayed by the NPs, was explained by the charge transfer between Au and H atoms. Transmittance Anisotropy Spectroscopy (TAS) technique permits to measure shifts of the LSPR as small as 0.02 nm upon H adsorption. It was shown that H_2 chemisorption occurs most likely directly on the Au NPs and an electron transfer from Au to H was observed, which eventually led to the decrease of the density of charge in the Au NPs and, consequently, yielded a redshift of the LSPR. Moreover, the proportionality of the intensity of the redshift was correlated with the areas of NPs with different particle sizes and it was shown that the dissociated H atoms migrate to the facets of the NPs, most likely the (100) facets, where they eventually recombine and desorb back to the gas phase [20]. Finally, the charge transfer induced by H adsorption at the atmospheric pressure of H_2 was calculated and the average negative charge transfer from every surface Au atom to H was found to be about -0.06 *e*, and the charge back-bonded localized on every Au–H bonding to be around -0.2 *e*. Consequently, their results showed a decrease of the electron population in the Au NP upon H adsorption, in line with some theoretical results [20]. For photocatalytic applications, gold nanoparticles have the

unique ability to perform chemical transformations at low operating temperatures and light intensities making these photocatalysts ideal for extended use in many chemical reactions by plasmon-induced and hot electron-based mechanisms [56-58].

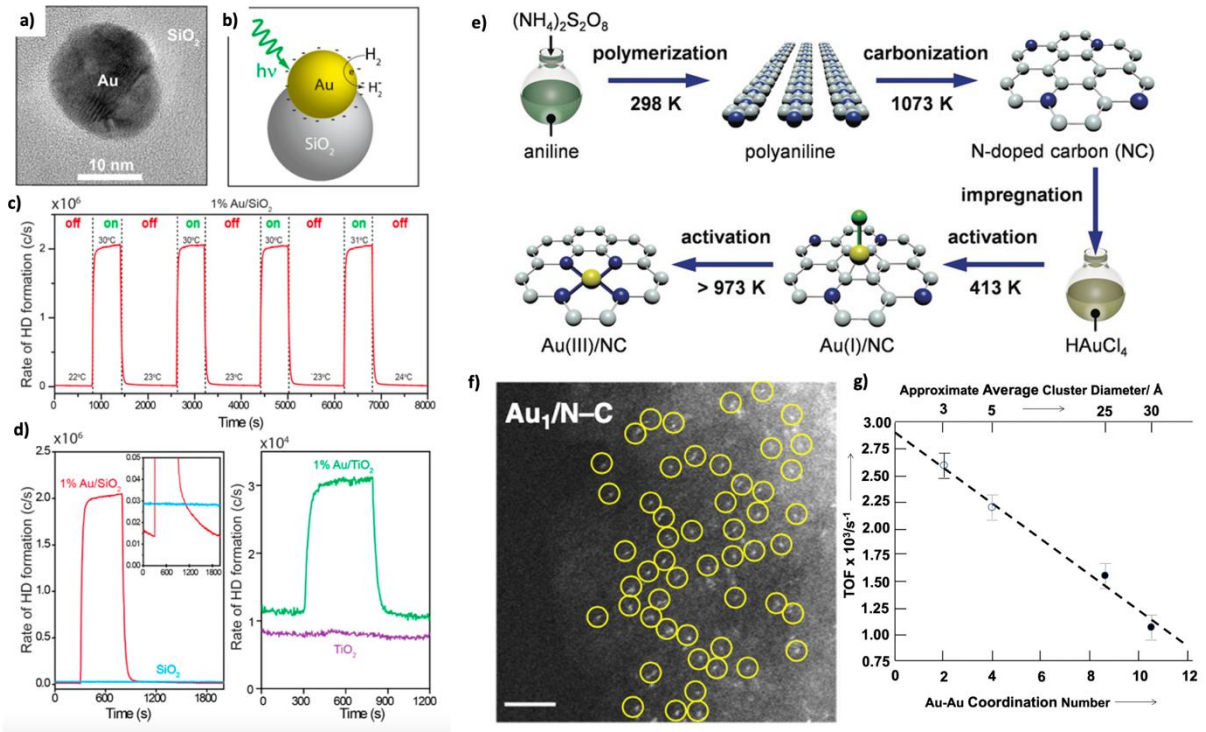

Figur3. *Hot-electron-induced dissociation of H_2/D_2 at room temperature (~23 °C) using 1% Au/SiO_2 photocatalyst. **(a)** High- resolution transmission electron micrograph of a single AuNP supported on SiO_2 matrix showing darker contrast of AuNP as compared to SiO_2 support. **(b)** Schematic representation of hot- electron-induced dissociation of H_2 on Au. **(c)** Real-time detection of rate of HD formation with laser excitation (2.4 W/cm^2, on) and without laser excitation (0.0 W/cm^2, off). Due to laser heating during 10 min of laser excitation, the temperature on the sample changes reversibly by 8 °C, as shown in the figure, from 22 to 30 °C. **(d)** A comparison of the rate of formation of HD using 1% Au/SiO_2 (left panel, red, inset showing the baseline of HD formation) and 1% Au/ TiO_2 (right panel, green) at the same experimental conditions and laser intensities (2.4 W/cm^2). No photocatalytic rate was observed with pristine SiO_2 (left panel, blue) and TiO_2 (right panel, purple). The diameters of the AuNPs were 5−30 nm. The excitation wavelength range is 450−1000 nm. Hydrogen spillover region identification [54]. **(e)** Synthetic steps involved in the preparation of nitrogen- doped carbon with a high density of electron- rich cavities, and incipient wetness impregnation with HAuCl4 in aqua regia, followed by thermal activation to create a gold-based single-atom catalyst. Au yellow, C gray, N blue, and Cl green. [51] **(f)** HAADF-STEM images of Au SACs (individual atoms highlighted with yellow circles, scale bar: 2 nm) [78]; **(g)** catalytic activity for ethene hydrogenation as a function of the Au–Au coordination number [74].*

To further demonstrate the efficiency of H_2 dissociation using Au/SiO_2 photocatalyst in direct comparison with the Au/TiO_2 previously used, the rate of photocatalytic HD formation was monitored on both Au/SiO_2 and Au/TiO_2. It was found the reaction rate in the presence of SiO_2 was enhanced by almost 2 orders of magnitude. The proposed mechanism was based on the generation of hot electrons by plasmon decay transfer to the H_2 molecules, substantially reducing the barrier for H_2 dissociation and the dielectric support plays a passive role in this reaction process. A plausible explanation was proposed for the substantially larger

dissociation rate in the presence of an SiO_2 relative to TiO_2 NP support based on the presence of a Schottky barrier at the AuNP/TiO_2 surface, which may facilitate hot-electron transfer into the TiO_2 matrix and therefore reducing the number of electrons available for the H_2 dissociation [54]. In addition, unlocking H_2 dissociation on gold surface via plasmonic nano-catalysis under visible light excitation opens the possibility for the development of selective hydrogenation catalysts. An increase in selectivity of the semi-hydrogenation of phenylacetylene was observed under visible light illumination using nanoparticle architectures comprised of Au or Au@Ag plasmonic core and ultrathin Pt-based catalytic shells [59]. The effective combination of plasmonic and catalytic properties allowed to enhance the catalytic transformation at the surface of the catalytic active but non-plasmonic metal (Pt), where the LSPR-excited hot carriers lead to the enhancement of activity and selectivity. It is worth to note that both positive (catalytic enhancement) and negative (reaction rate suppression) were found under visible-light illumination employing Au NPs supported on TiO_2 and SiO_2 as plasmonic catalysts for 4- nitrophenol hydrogenation. The nature of the reducing agent (H_2 and $NaBH_4$) and the occurrence of charge-transfer processes at the interface were responsible for the detected variations in plasmonic catalytic activities [60]. A significant enhancement in activity were found under plasmonic excitation for Au/SiO_2 NPs, whereas for Au/TiO_2 catalyst, a plasmonic enhancement was observed only for H_2(g) and a negative catalytic effect was observed for the reaction with BH_4^-(aq) as the reducing agent, due to charge-transfer of localized surface plasmon resonance-excited hot electrons from Au to TiO_2.

3.4. Cationic gold

An alternative approach for improving the activation of hydrogen is by using dispersed cationic gold species, which resemble the structure of traditional homogeneous catalysts [61-66]. As these metal species are immobilized in heterogeneous carriers, they are often described as single-atom catalysts (SACs), and they are attracting recently significant

interest in catalysis, because of the potential better utilization of the metal phase, **(Figure 4a)**, and excellent levels of selectivity, activity, stability [67-71]. Cationic gold single-atom catalyst (SACs) supported on multiwalled carbon nanotubes have been reported to be very active for the hydrogenation of 1,3-butadiene and 1-butyne in the presence of parahydrogen, an important catalytic process for the development of parahydrogen-induced polarization methods [72]. The Au SACs was found to be an order of magnitude more active and selective in pairwise hydrogen addition than the catalysts based on supported metal nanoparticle catalysts. Similarly, isolated Au species dispersed on iron oxide nanocrystallites (Au_1/FeO_x) were shown to be more sintering-resistant than Au nanostructures [73] for several hydrogenations [74-77]. Theoretical studies revealed that the positively-charged, surface-anchored Au^+ species formed covalent metal-support interactions, providing ultra-stability and remarkable catalytic performance. For example, it was shown that supported Au(III) species supported on MgO were responsible for inducing high activity and selectivity in ethene hydrogenation [74]. The It was also evidenced that the catalytic activity for ethene hydrogenation decreased as the Au–Au coordination number increased **(Figure 4 c)**. The data indicated that gold nanoparticles were less efficient catalysts for ethene hydrogenation, and that an atomic dispersion of the active phase is beneficial to drive the catalysis [74].

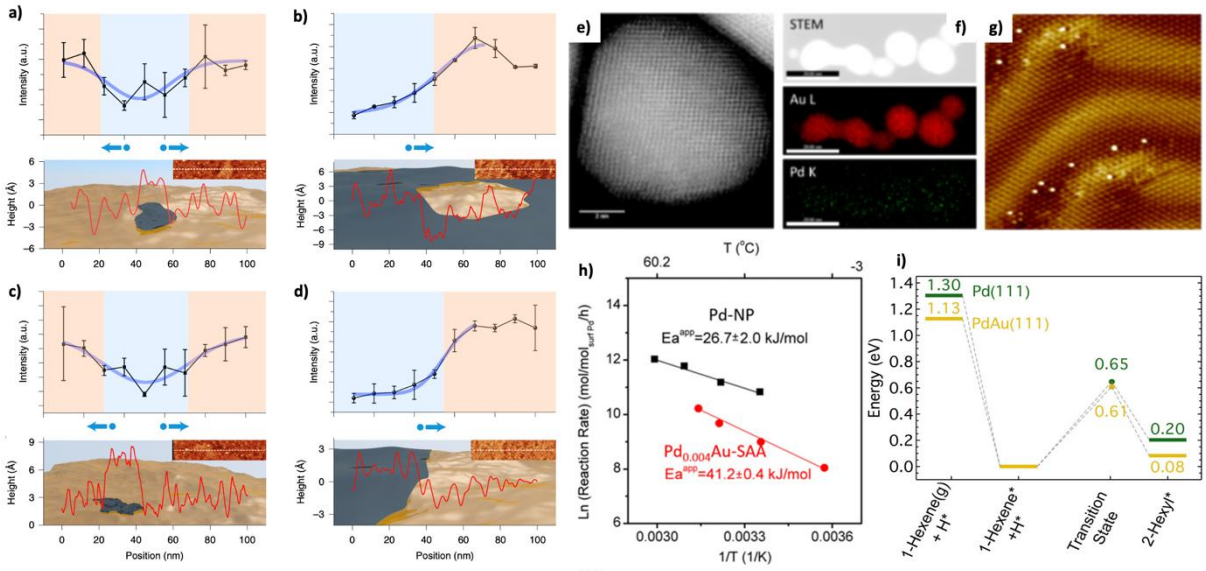

Figure 4. *Plots of the peak intensity of the 1,336 cm^{-1} mode in four different TErS line scan spectra extracted from the TErS map of a CNBT SAM on PdLC/Au (top images* ***a,c****) and on PdHC/Au (top images* ***b,d****) after exposure to H_2. Error bars indicate standard deviation for the two adjacent TErS line scans. The blue regions in the intensity plots indicate the reactive region defined by the FWHM of the fitted curves (purple trace).* ***a-d*** *bottom images: Topographic height profile (red line) of the surface along the dashed line of the inset of the corresponding STM images, superimposed with a schematic of the surface structure. Au, yellow shading; Pd, grey shading. The blue regions in the profile plots indicate the size of the Pd areas. Blue arrows with dots indicate the hydrogen spillover directions*. [94] *(e) STEM image of a $Pd_{0.004}$Au-single-atom alloy on SiO_2 nanoparticle (scale bar: 2 nm). (f) electron microscopy image with EDXS elemental maps. (g) STM image of the same single-allot catalyst collected with −300 mV bias and 900 pA current. (h) Arrhenius-type plot for 1-hexyne hydrogenation over Pd NPs and $Pd_{0.004}$Au-single-atom alloy on SiO_2. (i) DFT-calculated potential energy diagram comparing 1-hexene hydrogenation to 1-hexene desorption on Pd(111) and PdAu(111). Adsorbed species are denoted with an asterisk. Reprinted with permission from [95]*

The developments in single-atom catalysts have been possible due to advances in atomic-resolution microscopy that has imaged and documented the dispersed metal atoms and their evolution under reaction conditions [78-79]. However, the practical use of Au SACs is often compromised by (i) challenging synthesis protocols, using aqua regia as chlorine‑ based dispersing agent, and (ii) high catalyst susceptibility to sintering on non‑ functionalized carbon supports at > 500 K and/or under reaction conditions [51]. To address this challenge, a co-precipitation strategy to fabricate a series of gold single-atom supported metal organic framework catalysts has been reported [80]. Here, the metal was added during synthesis of the MOF precursors, intercalated through the layers *via* electrostatic surface interactions and replaced some of the anions (i.e., sulfate ion) present in the MOF structures. The presence of the gold atoms in isolated form was demonstrated by high-angle annular dark-field scanning transmission electron microscope and extended X-ray absorption fine structure spectroscopy. This approach recalls the copolymerization route for the immobilization of single atoms on graphitic carbon nitrides [81-82]. Alternatively, a dry ball milling synthetic protocol for the kg-scale production of Au_1/CeO_2 SACs was also reported [83]. This approach can be extended to prepare a family of oxide-supported noble metal SACs, which may pave a facile path for the mass production of oxide-supported cationic gold species for hydrogenations.

3.5. Alloying and bimetallic synergy

Another approach to facilitate H_2 dissociation and production of weakly bound H atoms is by exploiting gold alloying [84-86]. The alloy combination includes a catalytic metal

that exhibits facile H_2 dissociation and a coinage metal that can utilize the weakly bound H atoms to catalyze hydrogenation reactions [87-88]. One of the most promising bimetallic catalysts for hydrogenation are Au-Pd nanoparticles either in alloyed or core-shell structure [89]. For H_2 activation on Pd−Au, the necessary ensemble size has been debated. It was concluded that the presence of contiguous Pd atoms is essential for H_2 activation [90].

An atomic-level understanding of reactive sites for H_2 activation in Pd-Au alloys can elucidate the minimal Pd ensemble capable of activating H_2 and reveal the energetic landscape for uptake, spillover, and release of H. These steps were investigated with the aid of scanning tunneling microscopy (STM), temperature-programmed desorption (TPD), and DFT. Using well-defined Pd−Au model surfaces, it was demonstrated that Pd monomers in a Au(111) surface are responsible for activating H_2. By coupling high-resolution STM with TPD it was demonstrated that low concentrations of individual, isolated Pd atoms can dissociate H_2 due to the fact that the concentration of adsorbed H atoms is proportional to the surface concentration of Pd atoms in Au. Combining TPD with DFT, it was further elucidated the energetic landscape for H_2 adsorption, activation, and desorption from isolated Pd atoms, revealing (i) a low-temperature pathway for H_2 activation and (ii) release through the Pd atoms with minimal spillover to Au.

To carry out spatially resolved investigation [91-93] for revealing the mechanism of the catalytic selective hydrogenation of chloronitrobenzene to chloroaniline, a number of spectroscopic techniques were utilized, such as tip-enhanced Raman spectroscopy (TERS) on well-defined Pd(submonoayer)/Au(111) bimetallic catalysts, where the surface topography and chemical fingerprint information could be mapped with high accuracy and simultaneously with nanoscale resolution of ~10 nm. TERS imaging of the surface after catalytic hydrogenation showed that the reaction occurred beyond the location of Pd sites. The results demonstrated that in the case of hydrogen spillover after dissociation of hydrogen molecules

on Pd, adsorbed hydrogen atoms diffused onto the adjacent Au surfaces (spillover) and initiated the hydrogenation, therefore hydrogenation took place extend beyond the Pd areas and onto the Au areas **(Figures 5 e-l)**. Moreover, the evidence that hydrogenation due to spillover of adsorbed hydrogen atoms occurs on Au over a distance of ~15–30 nm from the Pd catalytic sites was provided [45]. To better understand the mechanisms of the reaction for the proposed reaction DFT confirmed the feasibility of the diffusion of hydrogen atoms from Pd to the neighboring Au area and provide a plausible explanation for the high chemoselectivity observed on Pd/Au model system [94].

The ultimate limit of the ensemble size in metal alloys corresponds to the case of single atom alloys (SAAs), where atomically-dispersed metal atoms facilitating the activation of hydrogen are entrapped and dispersed on the surface of a host metal, participating more in the adsorption of the activated H species and reaction cycle. Such materials have also drawn increased interest owing to their potential ability to break linear scaling relationships in alloy catalysis. Here, Au is a highly selective hydrogenation catalyst, but it is not active at low temperatures. Through measurements of reaction kinetics and in operando spectroscopy studies, the facile activation of hydrogen on PdAu SAAs was followed, involving the splitting of molecular hydrogen by the palladium sites and then reaction of the adsorbed H species on gold [95]. This also limits over-hydrogenation and oligomerization side reactions. Similarly, the addition of a small amount of Ni on either supported or unsupported Au surfaces induces resistance to sintering, along with a beneficial effect on the catalytic activity in the selective dehydrogenation of ethanol to acetaldehyde and hydrogen.

Differently from alloys, in bimetallic nanoparticles the chemical composition and order affect the catalytic properties of bimetallic systems [96]. The incorporation of the second metal can also help to overcome the limitations observed for monometallic nanoparticles.

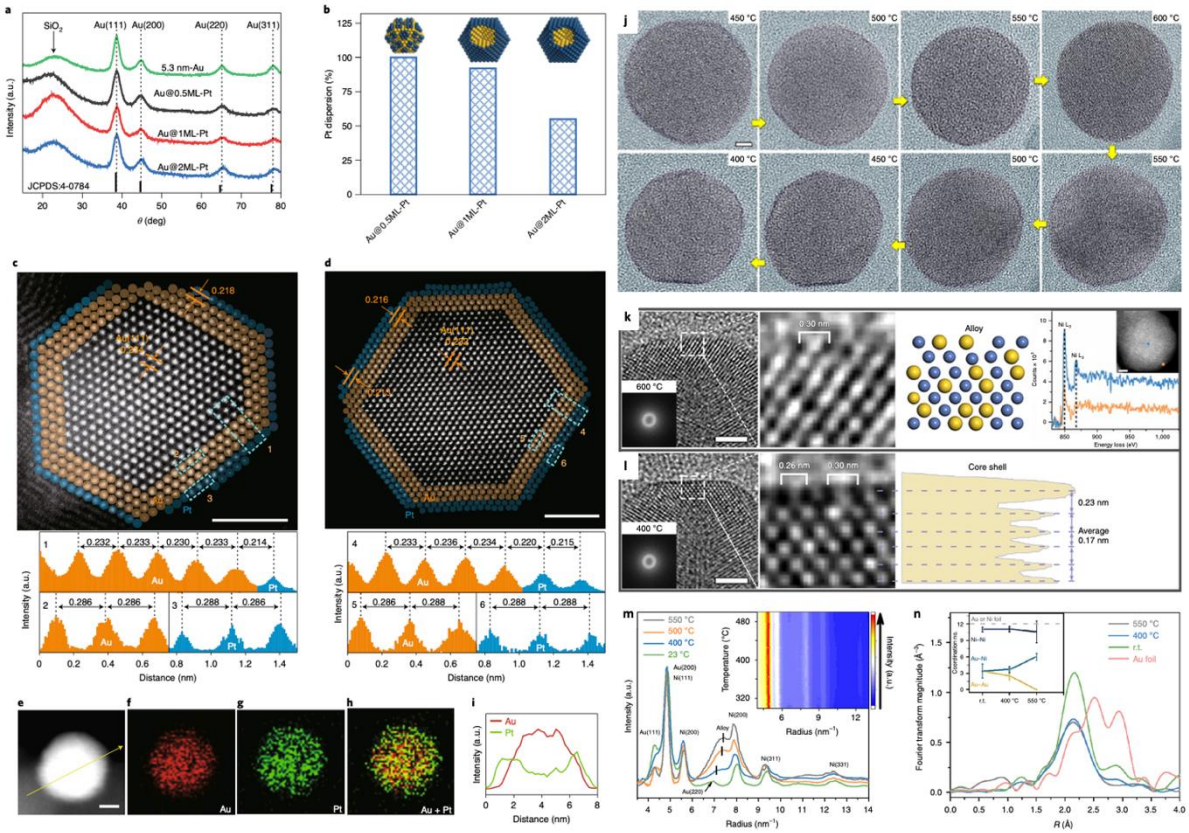

***Figure 5**. Morphology of Au@Pt core–shell catalysts. **a**, X-ray diffraction spectra of 5.3 nm-Au and Au@Pt bimetallic catalysts. **b**, Platinum dispersions of Au@Pt bimetallic catalysts as determined by CO chemisorption. The insets show the models of the corresponding Au@Pt core–shell catalysts, where the dark blue and yellow spheres are platinum and gold atoms, respectively. **c**,**d**, Representative atomic-resolution HAADF-STEM images of Au@1ML-Pt (**c**) and Au@2MLPt (**d**) catalysts, with the corresponding line intensity profiles along the numbered dashed rectangles to show the interplanar distance and the lattice distance. In **c** and **d**, the atoms in the outer layers are shown as light yellow and blue spheres to highlight the gold core and platinum shell. **e**–**h**, A STEM image of an Au@2ML-Pt particle (**e**) and the corresponding EDS mapping of Au (**f**), Pt (**g**), and Au + Pt (**h**) signals. **i**, Line profile of Au@2ML-Pt. The yellow arrow in **e** indicates the position for the line profile in **i**. The length of the scale bars in **c**, **d**, **e** are 2 nm. **j**, In situ TEM imaging of the alloying and dealloying evolution of an individual NiAu particle during the CO_2 hydrogenation reaction. Scale bar, 2 nm. **k,l**, Surface atom arrangement of a NiAu NP reconstructed from the full alloy (600 °C) (**k**) to the Ni@Au core–shell (400 °C) (**l**); the four parts from left to right in **k** show the high-resolution transmission electron microscopy (HRTEM) image (with a Thon ring inset), the corresponding enlargement of the surface area, schematic structure and point analysis of the electron energy loss spectra (with a HAADF inset); the three parts from left to right in **c** show the HRTEM image (with a Thon ring inset), the corresponding enlargement of the surface area and phase contrast profile. Scale bars, 2 nm. **m**, Intensity profiles from the integration of diffraction rings of selected area electron diffraction (SAED) patterns during the reaction. The inset shows 2D profiles stacking along with reaction temperature. **n**, In situ EXAFS of the Au L_3 edge and coordination number changes (inset) of the Au–Au, Au–Ni and Ni–Ni pairs at room temperature (r.t.), 400 and 550 °C. The microstructural evolution during the catalytic reaction for the reconstruction from the Ni@Au core–shell to the NiAu alloy is evidenced through atomic scale microscopy (TEM/STEM and SAED) as well as the overall statistics of the spectroscopy (EXAFS and FTIR). a.u., arbitrary units. Reprinted with permission from [23] [97]*

By using DFT it was predicted that to overpass this limitation from the size dependent relationship on monometallic Pt catalysts, a bimetallic monolayer platinum on Au catalyst could lead to higher activity as well as to higher selectivity. Therefore, core-shell bimetallic Au@Pt/SiO_2 catalyst with a monolayer (ML) platinum shell, by using atomic layer deposition (ALD) methodology were also studied. In addition, the catalytic activity with a range of bimetallic Au-Pt catalysts using 0.5, 1 and 2 ML platinum shells, with 1 ML of platinum shell

to show the highest activity of *para*-chloronitrobenzene and selectivity to *para*-chloroaniline were compared **(Figures 5 a-i)**. The enhanced activity of the Au@Pt/SiO_2 catalyst with a monolayer (ML) platinum shell was attributed to the enhanced charge transfer from gold to platinum atoms and the presence of a considerable ligand effect and lattice stretch of the platinum shell induced by the gold core that substantially shifts the platinum shell d-band center toward the Fermi level, while preserving the terrace sites for high selectivity as shown by DFT studies [23].

Finally, the catalyst showed excellent stability with respect to the monometallic Pt catalyst that suffer from agglomeration and leaching of Pt particles and chlorine poisoning [23]. Au-based bimetallic catalysts were also shown to possess excellent activity for the CO_2 hydrogenation to CO. Ni-Au bimetallic catalytic systems based on core-shell methodology were found very active in this reaction. SiO_2 was chosen as a support and the typical structure of the synthesized core-shell nanoparticles, consisted of a face-centered cubic Ni core, and 2-3 atomic layers of an ultrathin gold shell. Catalytic studies showed a high selectivity to CO (95%) with conversion level between 4.5-18% and temperature range of 340-600 °C and ex-situ STEM characterization showed the presence of core-shell structure, (ultrathin gold shell). However, during *in situ* STEM imaging, a phase transition from the Ni@Au core-shell to a NiAu alloy at similar reaction temperatures was observed. *In situ* TEM analysis was performed and revealed that during the heat treatment from 450 to 600 °C the Au species at the outmost surface were dissolved in the Ni matrix forming a mixed NiAu alloy [97]. During the cooling process to 450-500 °C, the recovery of the Ni@Au core shell structure occurred. To support their evidence reconstruction details of the NiAu surface were additionally monitored during the recovery process from the NiAu alloy to the Ni@Au core-shell **(Figures 5 j-n)**. Moreover, control experiments using a gas-cell reactor were carried out, which allowed simultaneous imaging under a 1 bar reaction environment to minimize the ‘pressure

gap' between the in situ environmental TEM experiments (~9 mbar) and the actual reaction conditions (1 bar) and they reproduced the reaction-driven alloying of NiAu NPs, which confirmed the credibility of their original TEM results. These results were further confirmed by in situ XAS and in situ FTIR studies. In addition, the DFT studies revealed the most energetically favored reaction pathway, which consisted of two stages. The first one was the hydrogenation of CO_2 to form the adsorbed CO and in the second stage, the most energetically favored reaction pathway was the diffusion of the adsorbed CO from the Ni site onto the Au site and finally the desorption of CO. These results conclude that the surface Ni atoms offer the active sites for the hydrogenation of CO_2 and the surface Au atoms are responsible for the selective production of CO [97].

4. Summary and Outlook

The results reported so far demonstrated that gold-based catalysts remain promising catalysts for selective hydrogenation reactions. However, catalytic hydrogenations are molecularly complex in nature and four key parameters can affect the reaction: light assistance, size of the metal, interaction between the metal and the support, and the presence of ligands or modifiers on the metal surface. All these parameters strongly influence the hydrogen activation pathway. Depending on the activation mode (homolytic scission to H atoms, and heterolytic scission into H^+/H^- pairs), different degrees of efficiency in the catalytic process can be expected. For example, it was demonstrated that the presence of some organic linkers at the gold surface is necessary to perform selective hydrogenations due to the heterolytic scission.

The control of the sintering tendency of Au species during reaction together with the low solvent tolerance of these catalysts remains to date an important challenge. Research works are being devoted towards the search for appropriate promoters and components able to

improve the catalytic performance of Au-based catalysts. The shift from the use of gold nanoparticles towards cationic gold single atoms seems to improve the catalysts durability and open new ways for the regeneration of the catalytic materials [98].

Another important challenge will be the use of hybrid catalysts mixing single atoms and nanoscale particles. In this case cascade reactions can be performed or reaction rate can be significantly improved. This could be very interesting in the hydrogen involved reaction as the hydrogen dissociation and reactivity is strongly correlated to the size of gold.

Finally, the fundamental understanding of the reaction mechanisms still requires further investigation as it can provide practical information for the rational design of catalysts. To understand the catalyst reduction process, the determination of the formation of intermediates, by exploiting advanced *in-situ* characterization techniques, are required. However, experiments and DFT simulations need to be combined to understand the adsorption/desorption process and to explain the selectivity path to a specific product.

References:

[1] Vogt, C., Weckhuysen, B.M. The concept of active site in heterogeneous catalysis. *Nat Rev Chem* **6**, 89–111 (2022). https://doi.org/10.1038/s41570-021-00340-y

[2] Navarro-Jaén, S., Virginie, M., Bonin, J. *et al.* Highlights and challenges in the selective reduction of carbon dioxide to methanol. *Nat Rev Chem* **5**, 564–579 (2021). https://doi.org/10.1038/s41570-021-00289-y

[3] Shuo, Ch., Wojcieszak, R., Dumeignil, F., Marceau, E., Royer, S. How Catalysts and Experimental Conditions Determine the Selective Hydroconversion of Furfural and 5-Hydroxymethylfurfural. *Chem. Rev.*, **118**, 11023-11117 (2018). https://doi.org/10.1021/acs.chemrev.8b00134

[4] Zugic, B., Wang, L., Heine, C. *et al.* Dynamic restructuring drives catalytic activity on nanoporous gold–silver alloy catalysts. *Nature Mater* **16**, 558–564 (2017). https://doi.org/10.1038/nmat4824

[5] Lemire, C., Meyer, R., Shaikhutdinov, S. & Freund, H-J. Do quantum size effects control CO adsorption on gold nanoparticles? *Angew. Chem. Int. Edn*. **43**, 118–121 (2003). https://doi.org/10.1002/anie.200352538

[6] Hvolbæk, B. et al. Catalytic activity of Au nanoparticles. *Nano Today* **2**, 14–18 (2007). https://doi.org/10.1016/S1748-0132(07)70113-5

[7] Fujita, T., Guan, P., McKenna, K. *et al.* Atomic origins of the high catalytic activity of nanoporous gold. *Nature Mater* **11**, 775–780 (2012). https://doi.org/10.1038/nmat3391

[8] Wang, H., Wang, L., Lin, D. *et al.* Strong metal–support interactions on gold nanoparticle catalysts achieved through Le Chatelier's principle. *Nat Catal* **4**, 418–424 (2021). https://doi.org/10.1038/s41929-021-00611-3

[9] Lopez, N. et al. On the origin of the catalytic activity of gold nanoparticles for low-temperature CO oxidation. *J. Catal.* **223**, 232–235 (2004). https://doi.org/10.1016/j.jcat.2004.01.001

[10] Haruta, M., When Gold Is Not Noble: Catalysis by Nanoparticles. *Chem. Rec*., **3**, 75–87 (2003). https://doi.org/10.1002/tcr.10053

[11] Corma A., Garcia, H., Supported gold nanoparticles as catalysts for organic reactions. *Chem. Soc. Rev*. **37**, 2096-2126 (2008). https://doi.org/10.1039/B707314N

[12] Bond, G.C. Hydrogenation by gold catalysts: an unexpected discovery and a current assessment. *Gold Bull* **49**, 53–61 (2016). https://doi.org/10.1007/s13404-016-0182-8

[13] Delgado, J.A., Godard, C. (2020). Progress in the Selective Semi-hydrogenation of Alkynes by Nanocatalysis. In: van Leeuwen, P., Claver, C. (eds) Recent Advances in Nanoparticle Catalysis. Molecular Catalysis, vol 1. Springer, Cham. https://doi.org/10.1007/978-3-030-45823-2_10

[14] Hutchings, G., Heterogeneous Gold Catalysis. *ACS Cent. Sci.* **4**, 1095–1101, (2018). https://doi.org/10.1021/acscentsci.8b00306

[15] Bus, E., Miller, J.T., van Bokhoven, J.A., Hydrogen Chemisorption on Al_2O_3-Supported Gold Catalysts. *J. Phys. Chem. B*, **109**, 14581–14587 (2005). https://doi.org/10.1021/jp051660z

[16] Fujitani, T., Nakamura, I., Akita, T., Okumura, M., Haruta, M., Hydrogen Dissociation by Gold Clusters. *Angew. Chem., Int. Ed.*, **48**, 9515–9518 (2009). https://doi.org/10.1002/anie.200905380

[17] Green, I.X., Tang, W., Neurock, M., Yates, J.T., Low-Temperature Catalytic H_2 Oxidation over Au Nanoparticle/TiO_2 Dual Perimeter Sites. *Angew. Chem., Int. Ed.*, **50**, 10186–10189 (2011). https://doi.org/10.1002/anie.201101612

[18] Manzoli, M., Chiorino, A., Vindigni, F., Boccuzzi, F., Hydrogen interaction with gold nanoparticles and clusters supported on different oxides: A FTIR study. *Catal. Today*, **181**, 62–67 (2012). https://doi.org/10.1016/j.cattod.2011.07.029
[19] Boronat, M., Concepcion, P., Corma, A., Unravelling the Nature of Gold Surface Sites by Combining IR Spectroscopy and DFT Calculations. Implications in Catalysis. *J. Phys. Chem. C*, **113**, 16772–16784 (2009). https://doi.org/10.1021/jp905157r
[20] Watkins, W.L., Borensztein, Y., Mechanism of hydrogen adsorption on gold nanoparticles and charge transfer probed by anisotropic surface plasmon resonance. *Phys.Chem.Chem.Phys*., **19**, 27397-27405 (2017). https://doi.org/10.1039/C7CP04843B
[21] Hammer, B., Norskov, J. Why gold is the noblest of all the metals. *Nature* **376**, 238–240 (1995). https://doi.org/10.1038/376238a0
[22] Sun, X., Dawson, S.R., Parmentier, T.E. *et al.* Facile synthesis of precious-metal single-site catalysts using organic solvents. *Nat. Chem.* **12**, 560–567 (2020). https://doi.org/10.1038/s41557-020-0446-z
[23] Guan, Q., Zhu, C., Lin, Y. *et al.* Bimetallic monolayer catalyst breaks the activity–selectivity trade-off on metal particle size for efficient chemoselective hydrogenations. *Nat Catal* **4**, 840–849 (2021). https://doi.org/10.1038/s41929-021-00679-x
[24] Chmielewski, A., et al. Reshaping Dynamics of Gold Nanoparticles under H_2 and O_2 at Atmospheric Pressure. *ACS Nano*, **13 (2)**, 2024-2033, (2019). https://doi.org/10.1021/acsnano.8b08530
[25] Bai, S.T., De Smet, G., Liao, Y., et al: Homogeneous and heterogeneous catalysts for hydrogenation of CO_2 to methanol under mild conditions. *Chemical Society Reviews*, **50**, 4259-4298 (2021). https://doi.org/10.1039/D0CS01331E
[26] Gesesse D., Wang, C., Chang Bor, K., Tai S-H., et al. A soft-chemistry assisted strong metal–support interaction on a designed plasmonic core–shell photocatalyst for enhanced photocatalytic hydrogen production. Nanoscale, **12**, 7011-7023 (2020). https://doi.org/10.1039/C9NR09891G
[27] Ferraz P, C., Navarro-Jaén, S., Rossi, L., et al. Enhancing the activity of gold supported catalysts by oxide coating: towards efficient oxidations. *Green Chemistry*, **23**, 8453-8457, (2021). https://doi.org/10.1039/D1GC02889H
[28] Nguyen, K.T., Hiep Vuong, V., Nguyen, T.N. *et al.* Unusual hydrogen implanted gold with lattice contraction at increased hydrogen content. *Nat Commun* **12**, 1560 (2021). https://doi.org/10.1038/s41467-021-21842-9
[29] Martín, A.J., Mitchell, S., Mondelli, C. *et al.* Unifying views on catalyst deactivation. *Nat Catal* **5**, 854–866 (2022). https://doi.org/10.1038/s41929-022-00842-y
[30] Segura, Y., Lopez, N., Perez-Ramirez, J., Origin of the superior hydrogenation selectivity of gold nanoparticles in alkyne + alkene mixtures: Triple- versus double-bond activation. *J Catal.* **247,** 383-386 (2007). https://doi.org/10.1016/j.jcat.2007.02.019
[31] van Deelen, T. W., Hernández Mejía, C. de Jong, K. P. Control of metal-support interactions in heterogeneous catalysts to enhance activity and selectivity. *Nat. Catal.* **2**, 955–970 (2019). https://doi.org/10.1038/s41929-019-0364-x
[32] Vijay, S., Ju, W., Brückner, S. *et al.* Unified mechanistic understanding of CO_2 reduction to CO on transition metal and single atom catalysts. *Nat Catal* **4**, 1024–1031 (2021). https://doi.org/10.1038/s41929-021-00705-y
[33] Nørskov, J., Bligaard, T., Rossmeisl, J. *et al.* Towards the computational design of solid catalysts. *Nature Chem* **1**, 37–46 (2009). https://doi.org/10.1038/nchem.121
[34] Milone, C., Ingoglia, R., Pistone, A., Neri, G., Frusteri, F., Galvagno, S., Selective hydrogenation of *α,β*-unsaturated ketones to *α,β*-unsaturated alcohols on gold-supported catalysts. *J. Catal.* **222**, 348-356 (2004). https://doi.org/10.1016/j.jcat.2003.11.003

[35] Fiorio, J., Rossi, L. Clean protocol for deoxygenation of epoxides to alkenes *via* catalytic hydrogenation using gold. *Catal. Sci. Technol.*, **11**, 312-318 (2021). https://doi.org/10.1039/d0cy01695k
[36] Liang, S., Hammond, G.B., Xu, B., Supported gold nanoparticles catalyzed cisselective semihydrogenation of alkynes using ammonium formate as the reductant. *Chem. Commun*. **52**, 6013—6016 (2016). https://doi.org/10.1039/C6CC01318J
[37] Fiorio, J., Gonçalves, R.V., Teixeira-Neto, E., et al. Accessing Frustrated Lewis Pair Chemistry through Robust Gold@N-Doped Carbon for Selective Hydrogenation of Alkynes. *ACS Catal.* **8(4)**, 3516–3524 (2018). https://doi.org/10.1021/acscatal.8b00806
[38] Stephan, D., The broadening reach of frustrated Lewis pair chemistry. *Science*, **354**, aaf7229 (2016). https://doi/10.1126/science.aaf7229
[39] Fiorio, J., Lopez, N., Rossi, L., Gold–Ligand-Catalyzed Selective Hydrogenation of Alkynes into *cis*-Alkenes via H_2 Heterolytic Activation by Frustrated Lewis Pairs. *ACS Catal.* **7(4)**, 2973–2980 (2017). https://doi.org/10.1021/acscatal.6b03441
[40] Almora-Barrios, N., Cano, I., van Leeuwen, P., Lopez, N., Concerted Chemoselective Hydrogenation of Acrolein on Secondary Phosphine Oxide Decorated Gold Nanoparticles. *ACS Catal.* **7(6)**, 3949–3954 (2017). https://doi.org/10.1021/acscatal.7b00355
[41] Lu, G., Zhang, P., Sun, D., et al. Gold catalyzed hydrogenations of small imines and nitriles: enhanced reactivity of Au surface toward H_2 *via* collaboration with a Lewis base. *Chem. Sci.*, **5**, 1082-1090 (2014). https://doi.org/10.1039/C3SC52851K
[42] Lv, X., Lu, G., Wang, Z.Q., et al. Computational Evidence for Lewis Base-Promoted CO_2 Hydrogenation to Formic Acid on Gold Surfaces. *ACS Catal.* **7(7)**, 4519–4526 (2017). https://doi.org/10.1021/acscatal.7b00277
[43] Ren, D.; He, L.; Yu, L.; Ding, R.-S.; et al. An Unusual Chemoselective Hydrogenation of Quinoline Compounds Using Supported Gold Catalysts. *J. Am. Chem. Soc*. **134**, 17592−17598 (2012). https://doi.org/10.1021/ja3066978
[44] Lu, G.; Zhang, P.; Sun, D.; Wang, L.; et al. Gold Catalyzed Hydrogenations of Small Imines and Nitriles: Enhanced Reactivity of Au Surface toward H2 via Collaboration with a Lewis Base. *Chem. Sci*. *5*, 1082−109 (2014). https://doi.org/10.1039/C3SC52851K
[45] Cano, I.; Chapman, A. M.; Urakawa, A.; van Leeuwen, P. W. N. M. Air-Stable Gold Nanoparticles Ligated by Secondary Phosphine Oxides for the Chemoselective Hydrogenation of Aldehydes: Crucial Role of the Ligand. *J. Am. Chem. Soc*. **136**, 2520−2528 (2014). https://doi.org/10.1021/ja411202h
[46] Cano, I.; Huertos, M. A.; Chapman, A. M.; Buntkowsky, G.; Gutmann, T.; Groszewicz, P. B.; van Leeuwen, P. W. N. M. Air-Stable Gold Nanoparticles Ligated by Secondary Phosphine Oxides as Catalyst for the Chemoselective Hydrogenation of Substituted Aldehydes: a Remarkable Ligand Effect. *J. Am. Chem. Soc*. **137(5)**, 7718−7727 (2015). https://doi.org/10.1021/ja411202h
[47] Garcia-Melchor, M., Lopez, N., Homolytic Products from Heterolytic Paths in H_2 Dissociation on Metal Oxides: The Example of CeO_2. *J. Phys. Chem. C*, **118(20)**, 10921–10926 (2014). https://doi.org/10.1021/jp502309r
[48] Hoffmann-Röder, A.; Krause, N. The golden gate to catalysis. *Org. Biomol. Chem*. **3**, 387-391 (2005). https://doi.org/10.1039/B416516K
[49] Lyalin, A., Taketsugu, T., A computational investigation of H_2adsorption and dissociation on Au nanoparticles supported on TiO_2 surface. *Faraday Discuss.*, 152, 185-201 (2011). https://doi.org/10.1039/C1FD00013F
[50] Whittaker, T., Kumar, S., Peterson, Ch., et al. H_2 Oxidation over Supported Au Nanoparticle Catalysts: Evidence for Heterolytic H_2 Activation at the Metal–Support Interface. *J. Am. Chem. Soc.* **140(48)**, 16469–16487 (2018). https://doi.org/10.1021/jacs.8b04991

[51] Lin, R., Albani, D., Fako, E., Kaiser, S., et al. Design of Single Gold Atoms on Nitrogen-Doped Carbon for Molecular Recognition in Alkyne Semi-Hydrogenation. *Angew. Chim. Int. Ed.* **58**, 504-509 (2019). https://doi.org/10.1002/anie.201805820
[52] Du, X., Huang, Y., Pan, X. *et al.* Size-dependent strong metal-support interaction in TiO_2supported Au nanocatalysts. *Nat Commun* **11**, 5811 (2020). https://doi.org/10.1038/s41467-020-19484-4
[53] Sun, Y., Cao, Y., Wang, L. *et al.* Gold catalysts containing interstitial carbon atoms boost hydrogenation activity. *Nat Commun* **11**, 4600 (2020). https://doi.org/10.1038/s41467-020-18322-x
[54] Mukherjee, S., Zhou, L., Goodman, A. et al., Hot-Electron-Induced Dissociation of H_2 on Gold Nanoparticles Supported on SiO_2. *J. Am. Chem. Soc.* **136**, 64−67 (2014). https://doi.org/10.1021/ja411017b
[55] Mukherjee, S., Libisch, F. Large, N., et al., Hot Electrons Do the Impossible: Plasmon-Induced Dissociation of H_2 on Au. *Nano Lett.* **13(1)**, 240–247 (2013). https://doi.org/10.1021/nl303940z
[56] Christopher, P., Xin, H., Marimuthu, A. *et al.* Singular characteristics and unique chemical bond activation mechanisms of photocatalytic reactions on plasmonic nanostructures. *Nature Mater* **11**, 1044–1050 (2012). https://doi.org/10.1038/nmat3454
[57] Linic, S.; Christopher, P.; Xin, H.; Marimuthu, A. Catalytic and Photocatalytic Transformations on Metal Nanoparticles with Targeted Geometric and Plasmonic Properties. *Acc. Chem. Res*. **46**, 1890-1899 (2013). https://doi.org/10.1021/ar3002393
[58] Brus, L. Noble Metal Nanocrystals: Plasmon Electron Transfer Photochemistry and Single-Molecule Raman Spectroscopy. *Acc. Chem. Res*. **41**, 1742-1749 (2008). https://doi.org/10.1021/ar800121r
[59] Quiroz, J.; Barbosa, E.; Araujo, T., Fiorio, J.; et al. Controlling Reaction Selectivity over Hybrid Plasmonic Nanocatalysts. *Nano Lett.* **18**, 7289−7297 (2018). https://doi.org/10.1021/acs.nanolett.8b03499
[60] Barbosa, E., Fiorio, J., Mou, T.; Wang, B.; Rossi, L.; Camargo, P. Reaction Pathway Dependence in Plasmonic Catalysis: Hydrogenation as a Model Molecular Transformation. Chem. Europ. J. 24, 12330-12339 (2018). https://doi.org/10.1002/chem.201705749
[61] Pyykkö, P. Theoretical Chemistry of Gold. *Angew. Chem.* **43**, 4412-4456 (2004). https://doi.org/10.1002/anie.200300624
[62] Pyykkö, P. Relativity, Gold, Closed-Shell Interactions, and $CsAu{\cdot}NH_3$. *Angew. Chem. Int. Ed.* **41**, 3573-3578 (2002). https://doi.org/10.1002/1521-3773(20021004)41:19%3C3573::AID-ANIE3573%3E3.0.CO;2-R
[63] De Vos, D.; Sels, B. Gold Redox Catalysis for Selective Oxidation of Methane to Methanol. *Angew. Chem*. **117**, 30-32 (2005). https://doi.org/10.1002/ange.200461561
[64] Guzman, J.; Correttin, S.; Fierro-Gonzalez, J. et al. CO Oxidation Catalyzed by Supported Gold: Cooperation between Gold and Nanocrystalline Rare-Earth Supports Forms Reactive Surface Superoxide and Peroxide Species. *Angew. Chem. Int. Ed*. **44**, 4778-4781 (2005). https://doi.org/10.1002/anie.200500659
[65] Jones, C.; Taube, D.; Ziatdinov, V.; Periana, R.; Nielsen, R.; Oxgaard, J.; Goddard III, W. Selective Oxidation of Methane to Methanol Catalyzed, with C-H Activation, by Homogeneous, Cationic Gold. *Angew. Chem.* **116**, 4726-4729 (2004). https://doi.org/10.1002/ange.200461055
[66] Corma, A.; Gonzalez-Arellano, C.; Iglesias, M.; Sanchez, F. Gold Nanoparticles and Gold(III) Complexes as General and Selective Hydrosilylation Catalysts. Angew. Chem. Int. Ed. 119, 7966-7968 (2007). https://doi.org/10.1002/ange.200702032

[67] Wang, L., Guan, E., Zhang, J. *et al.* Single-site catalyst promoters accelerate metal-catalyzed nitroarene hydrogenation. *Nat Commun* **9**, 1362 (2018). https://doi.org/10.1038/s41467-018-03810-y
[68] Zhang, L., Ren, Y., at al. Single-atom catalyst: a rising star for green synthesis of fine chemicals. Nat. Sci. Rev., **5**, 653–672 (2018). https://doi.org/10.1093/nsr/nwy077
[69] Hannagan, R.T.; Giannakakis, G., Flytzani-Stephanopoulos, M., Sykes, E.Ch. Single-atom alloy catalysis. *Chem. Rev.* **120**, 12044–12088 (2020). https://doi.org/10.1021/acs.chemrev.0c00078
[70] Cui, X., Li, W., Ryabchuk, P. *et al.* Bridging homogeneous and heterogeneous catalysis by heterogeneous single-metal-site catalysts. *Nat Catal* **1**, 385–397 (2018). https://doi.org/10.1038/s41929-018-0090-9
[71] Cao, S., Yang, M., Elnabawy, A.O. *et al.* Single-atom gold oxo-clusters prepared in alkaline solutions catalyse the heterogeneous methanol self-coupling reactions. *Nat. Chem.* **11**, 1098–1105 (2019). https://doi.org/10.1038/s41557-019-0345-3
[72] Corma, A., Salnikov, O.G., Barskiy, D.A., Kovtunov, K.V. and Koptyug, I.V. Single-Atom Gold Catalysis in the Context of Developments in Parahydrogen-Induced Polarization. *Chem. Eur. J.*, **21**, 7012-7015 (2015). https://doi.org/10.1002/chem.201406664
[73] Qiao, B., Liang, JX., Wang, A. *et al.* Ultrastable single-atom gold catalysts with strong covalent metal-support interaction (CMSI). *Nano Res.* **8**, 2913–2924 (2015). https://doi.org/10.1007/s12274-015-0796-9
[74] Guzman, J.; Gates, B.C.; Structure and Reactivity of a Mononuclear Gold-Complex Catalyst Supported on Magnesium Oxide. *Angew. Chem.* **115**, 115-714 (2003). https://doi.org/10.1002/ange.200390159
[75] Comas-Vives, A.; Gonzalez- Arellano, C.; Corma, A.; Iglesias, M. ; et al. Single-Site Homogeneous and Heterogenized Gold(III) Hydrogenation Catalysts: Mechanistic Implications. *J. Am. Chem. Soc*. **128**, 4756-4765 (2006). https://doi.org/10.1021/ja057998o
[76] Zhang, X.; Shi, H.; Xu, B.; Catalysis by Gold: Isolated Surface Au^{3+} Ions are Active Sites for Selective Hydrogenation of 1,3-Butadiene over Au/ZrO_2 Catalysts. *Angew. Chem. Int. Ed*. 44, 7132-7135 (2005). https://doi.org/10.1002/anie.200502101
[77] Zhang, X.; Shi, H.; Xu, B.; Catalysis by Gold: Isolated Surface Au^{3+} Ions are Active Sites for Selective Hydrogenation of 1,3-Butadiene over Au/ZrO_2 Catalysts. Angew. Chem. 117, 7294-7297 (2005). https://doi.org/10.1002/ange.200502101
[78] He, X., He, Q., Deng, Y. *et al.* A versatile route to fabricate single atom catalysts with high chemoselectivity and regioselectivity in hydrogenation. *Nat Commun* **10**, 3663 (2019). https://doi.org/10.1038/s41467-019-11619-6
[79] Single atom catalysts push the boundaries of heterogeneous catalysis. *Nat Commun* **12**, 5884 (2021). https://doi.org/10.1038/s41467-021-26130-0
[80] Wang, Z., Gu, L., Song, L., Wang, H., Yu, R. Facile one-pot synthesis of MOF supported gold pseudo-single-atom catalysts for hydrogenation reactions. *Mater. Chem. Front.*, 2, 1024-1030 (2018). https://doi.org/10.1039/C8QM00081F
[81] Liu, J., Zou, Y., Cruz, D. et al. Ligand–Metal Charge Transfer Induced *via* Adjustment of Textural Properties Controls the Performance of Single-Atom Catalysts during Photocatalytic Degradation. *ACS Appl. Mater. Interf.* **13(22)**, 25858–25867 (2021). https://doi.org/10.1021/acsami.1c02243
[82] Vilé, G., Di Liberto, G., Tosoni, S., et al. Azide-Alkyne Click Chemistry over a Heterogeneous Copper-Based Single-Atom Catalyst. A*CS Catal.* **12(5)**, 2947–2958 (2022). https://doi.org/10.1021/acscatal.1c05610
[83] Gan, T., He, Q., Zhang, H. et al. Unveiling the kilogram-scale gold single-atom catalysts via ball milling for preferential oxidation of CO in excess hydrogen. *Chem. Eng. J.* **389**, 124490, (2020) https://doi.org/10.1016/j.cej.2020.124490

[84] Greeley, J., Mavrikakis, M. Alloy catalysts designed from first principles. *Nature Mater* **3**, 810–815 (2004). https://doi.org/10.1038/nmat1223
[85] Fu, Q., Luo, Y. Catalytic Activity of Single Transition-Metal Atom Doped in Cu(111) Surface for Heterogeneous Hydrogenation. *J. Phys. Chem. C* **117**, 14618−14624 (2013). https://doi.org/10.1021/jp403902g
[86] Alayoglu, S., Nilekar, A., Mavrikakis, M. *et al.* Ru–Pt core–shell nanoparticles for preferential oxidation of carbon monoxide in hydrogen. *Nature Mater* **7**, 333–338 (2008). https://doi.org/10.1038/nmat2156
[87] Kyriakou, G., Boucher, M. B., Jewell, A. D., Lewis, E. et al. Isolated Metal Atom Geometries as a Strategy for Selective Heterogeneous Hydrogenations. *Science* **335**, 1209-1212 (2012). https://doi.org/10.1126/science.1215864
[88] Boucher, M. B.; Zugic, B.; Cladaras, G.; et al. Single Atom Alloy Surface Analogs in $Pd_{0.18}Cu_{15}$ Nanoparticles for Selective Hydrogenation Reactions. *Phys. Chem. Chem. Phys*. **15**, 12187−12196 (2013). https://doi.org/10.1039/C3CP51538A
[89] Sankar, M., Dimitratos, N., Miedziak, P., et al. Designing bimetallic catalysts for a green and sustainable future. *Chem. Soc. Rev*., **41**, 8099-8139 (2012). https://doi.org/10.1039/C2CS35296F
[90] Maroun, F.; Ozanam, F.; Magnussen, O. M.; Behm, R. J. The Role of Atomic Ensembles in the Reactivity of Bimetallic Electrocatalysts. *Science* **293**, 1811−1814 (2001). https://doi.org/10.1126/science.1061696
[91] Venkatachalam, S., Jacob, T. Hydrogen Adsorption on Pd- Containing Au(111) Bimetallic Surfaces. *Phys. Chem. Chem. Phys*. **11(17)**, 3263-3270 (2009). https://doi.org/10.1039/B900250B
[92] Buurmans, I., Weckhuysen, B. Heterogeneities of individual catalyst particles in space and time as monitored by spectroscopy. *Nature Chem* **4**, 873–886 (2012). https://doi.org/10.1038/nchem.1478
[93] Sambur, J., Chen, TY., Choudhary, E. *et al.* Sub-particle reaction and photocurrent mapping to optimize catalyst-modified photoanodes. *Nature* **530**, 77–80 (2016). https://doi.org/10.1038/nature16534
[94] Yin, H., Zheng, LQ., Fang, W. *et al.* Nanometre-scale spectroscopic visualization of catalytic sites during a hydrogenation reaction on a Pd/Au bimetallic catalyst. *Nat Catal* **3**, 834–842 (2020). https://doi.org/10.1038/s41929-020-00511-y
[95] Liu, J., Uhlman, M., Montemore, M. *et al.* Integrated Catalysis-Surface Science-Theory Approach to Understand Selectivity in the Hydrogenation of 1-Hexyne to 1-Hexene on PdAu Single-Atom Alloy Catalysts. *ACS Catal.* ***9(9)****, 8757–8765 (2019)*
[96] Shi, D.; Sadier, A.; Girardon, J.S.; Mamede, A.S.; *et al.* Probing the core and surface composition of nanoalloy to rationalize its selectivity: Study of Ni-Fe/SiO2 catalysts for liquid-phase hydrogenation. *Chem Catal*. **2(7)**, 1686–1708 (2022). https://doi.org/10.1016/j.checat.2022.04.009
[97] Zhang, X., Han, S., Zhu, B. *et al.* Reversible loss of core–shell structure for Ni–Au bimetallic nanoparticles during CO_2 hydrogenation. *Nat Catal* **3**, 411–417 (2020). https://doi.org/10.1038/s41929-020-0440-2
[98] Datye, A.K., Guo, H. Single atom catalysis poised to transition from an academic curiosity to an industrially relevant technology. *Nat Commun.* **12**, 895 (2021). https://doi.org/10.1038/s41467-021-21152-0